

# Electronic structure and x-ray magnetic circular dichroism in (Ge,Mn)Te diluted magnetic semiconductors

V.N. Antonov<sup>1,2</sup>, A.P. Shpak<sup>1</sup>, L.V. Bekenov<sup>1</sup>, L.P. Germash<sup>3</sup>, A.N. Yaresko<sup>2</sup>

<sup>1</sup> Institute of Metal Physics of the National Academy of Sciences of Ukraine, 36 Vernadsky Str., 03142 Kiev, Ukraine

<sup>2</sup> Max-Planck-Institut für Festkörperforschung, Heisenbergstrasse 1, D–70569 Stuttgart, Germany

<sup>3</sup> National Technical University of Ukraine, Kiev Polytechnic Institute 14 Politechnichna Str., 03056 Kiev, Ukraine

Received December 25, 2009, in final form March 18, 2010

The electronic structure of the (Ge,Mn)Te diluted magnetic semiconductors was investigated theoretically from first principles, using the fully relativistic Dirac linear muffin-tin orbital (LMTO) band structure method. The electronic structure is obtained with the local spin-density approximation (LSDA) as well as the LSDA+*U* method. The x-ray magnetic circular dichroism (XMCD) spectra of (Ge,Mn)Te DMSs at the Mn *L*<sub>2,3</sub> edges are investigated theoretically from first principles. The origin of the XMCD spectra in the compound is examined. The calculated results are compared with available experimental data.

**Key words:** *electronic structure, diluted magnetic semiconductors, x-ray magnetic circular dichroism*

**PACS:** 71.28.+d, 71.25.Pi, 75.30.Mb

## 1. Introduction

The dilute magnetic semiconductors (DMS) are without doubt one of the most promising and interesting classes of magnetic materials. Their signature characteristic is carrier-mediated ferromagnetic exchange with which magnetic and electronic properties of microelectronic devices can be linked. Mn-doped III–V semiconductors are among the most frequently studied, particularly (Ga,Mn)As where the carrier-induced nature of the ferromagnetic exchange is well established (see, e.g. review papers [1, 2]). The nature of the electronic structure and magnetic exchange in other intensively studied III–V, II–VI or IV–VI systems is far from being understandable.

For the device application, DMSs should satisfy two requirements. One is carrier controllability and the second is Curie temperature ( $T_C$ ) higher than room temperature. III–V transition metals-based DMSs satisfy the first requirement. However, the highest Curie temperature reported so far for III–V DMSs except III–V nitrides is 170 K for (Ga,Mn)As [3]. DMSs films exhibit an extreme diversity of magnetic characteristics, depending on the method of preparation, heat treatment, additional doping, etc. The extreme sensitivity of the magnetic properties of these materials to the conditions of their preparation and annealing is due to a nonequilibrium distribution of defects arising during the preparation of the magnetic films.

Recently, Fukuma et al. have succeeded in the epitaxial growth of (Ge<sub>1-x</sub>Mn<sub>x</sub>)Te ferromagnetic films up to  $x = 0.96$  using an ionized cluster beam (ICB) technique [4]. Curie temperature  $T_C$  takes a maximum of 140 K at  $x = 0.51$  and the ferromagnetic order exists in the whole region of  $x \leq 0.96$ , though MnTe with  $x = 1$  limit is an antiferromagnetic compound. In addition, the magnetization clearly depends on the carrier concentration [5]. To understand ferromagnetism in (Ge<sub>1-x</sub>Mn<sub>x</sub>)Te, it is important to investigate its electronic structure, in particular, the Mn *3d* states.

Magnetic properties of IV–VI GeTe based diluted magnetic semiconductors with *3d* transition metals from Ti to Ni have been investigated by Fukuma et al. [6]. Ferromagnetic order was observed for the Cr, Mn, and Fe doped GeTe films, whereas the Ti, V, Co, and Ni doped films are

paramagnetic. The ferromagnetic order could give rise to  $p$ - $d$  exchange interaction because amplitudes of negative magnetoresistance and the anomalous Hall effect are proportional to that of spontaneous magnetization. The Curie temperatures determined by extrapolating the steep linear part of the temperature dependence of the squared residual magnetization for the Cr, Mn, and Fe doped GeTe films are 12, 47, and 100 K, respectively. Fukuma *et al.* [7] also investigated the ferromagnetic properties of IV–VI diluted magnetic semiconductor (Ge,Cr)Te and (Ge,Mn)Te films. The ferromagnetism in the (Ge,Cr)Te such as the spontaneous magnetization and the Curie temperature was found to be significantly affected by the stoichiometry, while the ferromagnetism of (Ge,Mn)Te films was hardly affected by the defects and strongly depended on the hole concentration. The difference could be ascribed to the interaction of the ferromagnetic order: short-range order such as a super-exchange mechanism plays a more important role than long-range order such as the Ruderman-Kittel-Kasuya-Yosida mechanism in the ferromagnetism of the (Ge,Cr)Te films.

Mn  $3d$  electronic structure in IV–VI ferromagnetic semiconductor  $(\text{Ge}_{1-x}\text{Mn}_x)\text{Te}$  ( $x = 0.32$ ) has been investigated by means of the soft X-ray magnetic circular dichroism measurements of the Mn  $2p-3d$  x-ray absorption spectra (XAS) [8]. The XAS and XMCD spectra show a characteristic feature of the localized  $\text{Mn}^{2+}$   $3d$  states. From the analysis of the spectra based on the configuration interaction theory, the parameters such as the  $p$ - $d$  hybridization and  $p$ - $d$  exchange constant were estimated. Mn  $L_{2,3}$  x-ray absorption and magnetic circular dichroism study has been also performed on ferromagnetic semiconductor  $(\text{Ge}_{1-x}\text{Mn}_x)\text{Te}$  with different Mn compositions  $x = 0.12, 0.32, 0.51,$  and  $1$  by Fukuma *et al.* [9]. The absorption and dichroism line shapes were found to be almost independent of the Mn composition, suggesting that the local chemical environment of Mn atoms is the same for (Ge,Mn)Te with the wide range of  $x$ . On the basis of the configuration interaction analysis for a  $\text{MnTe}_6$  cluster, the electronic structure parameters such as the  $p$ - $d$  hybridization and the  $p$ - $d$  exchange constant have been estimated. In order to investigate the Mn  $3d$  electronic structure in IV–VI ferromagnetic semiconductor  $(\text{Ge}_{1-x}\text{Mn}_x)\text{Te}$ , Senba *et al.* [10] have carried out the Mn  $3p$ - $3d$  resonant photoemission spectroscopy (RPES) and Mn  $L_3$  soft X-ray emission spectroscopy measurements. The Mn  $3d$  partial density of states derived from the RPES spectra indicate that the Mn  $3d$  states of  $(\text{Ge}_{1-x}\text{Mn}_x)\text{Te}$  are nearly localized with the divalent character.

Xie *et al.* theoretically investigated the electronic structure of (Ge,Mn)Te ferromagnetic diluted semiconductors with different compositions ( $x = 0.25, 0.5$  and  $0.75$ ) based on *ab initio* calculations within the local spin density approximation [11]. The electronic structure of  $3d$  transition metal doped GeTe was calculated by the pseudopotential method in the framework of a spin-polarized version of CASTEP. They present the theoretically calculated partial density of states (DOS) as well as  $E(\mathbf{k})$  curves.

In the present work we report a detailed theoretical investigation of the electronic structure, x-ray absorption and x-ray magnetic circular dichroism in IV–VI semiconductor GeTe with substitutional incorporation of Mn atoms on a Ge-site. This paper is organized as follows. Section 2 presents a description of the (Ge,Mn)Te crystal structure and the computational details. Section 3 is devoted to the electronic structure and x-ray circular and linear dichroism of the (Ge,Mn)Te DMS calculated in the fully relativistic Dirac LMTO band structure method. The calculated results are compared with the available experimental data. Finally, the results are summarized in section 4.

## 2. Crystal structure and computational details

Germanium telluride GeTe exists in cubic NaCl structure, a space group is  $Fm\bar{3}m$  (number 225) (Ge ions occupy the  $4a$  positions  $x = 0, y = 0, z = 0$ , and Te ions are placed at the  $4b$  sites  $x = 0.5, y = 0.5, z = 0.5$ ). Manganese telluride MnTe is crystallized in NiAs type crystal structure, a space group  $P63/mmc$  (number 194), (Mn ions occupy the  $2a$  positions  $x = 0, y = 0, z = 0$ , and Te ions are placed at the  $2c$  sites  $x = 0.3333, y = 0.6667, z = 0.25$ ) [12].

Our calculations of the electronic structure of the  $(\text{Ge}_{1-x}\text{Mn}_x)\text{Te}$  DMSs were performed for  $2a \times 2a \times 2a, 2a \times 2a \times a$  and  $2a \times a \times a$  supercells with one of Ge ions replaced by Mn. The supercell calculations were performed for compositions  $x = 0.03125$  (1/32),  $x = 0.0625$  (1/16),  $x =$

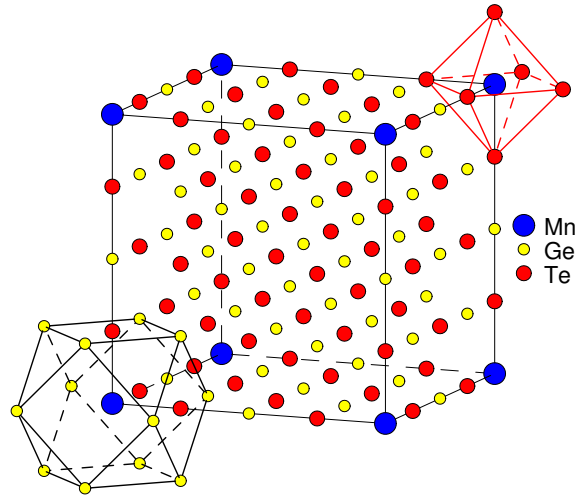


**Figure 1.** (Color online) Schematic representation of the  $(\text{Ge}_{1-x}\text{Mn}_x)\text{Te}$  structure for  $x = 0.03$ .

0.125 (1/8) and  $x = 0.5$  (1/2), using simple cubic  $Pm\bar{3}m$  (No. 221), simple tetragonal  $P4/mmm$  (No. 123), simple tetragonal  $P4/mmm$  (No. 123) and  $P63/mmc$  (No. 194) unit cells, respectively. The substitutional  $(\text{Ge}_{1-x}\text{Mn}_x)\text{Te}$  positions are illustrated in figure 1 for a 64-atom GeTe unit cell containing one substitutional  $\text{Mn}_{\text{Ge}}$  atom ( $x = 0.03125$ ). The  $\text{Mn}_{\text{Ge}}$  atom has six Te nearest neighbors at the distance of 3.0045 Å. The second coordinate sphere consists of 12 Ge atoms at the 4.249 Å distance.

We performed the geometry optimization of the  $(\text{Ge},\text{Mn})\text{Te}$  DMS using the pseudopotential VASP-SGGA method [13–15]. We optimized the internal freedom upon atoms with a fixed lattice constant, that is, the internal fractional coordinate was optimized. We found only a minor effect of the structure relaxation on the partial density of states in close vicinity of the Fermi level, while further away from the Fermi level the partial density of states did not change. The lattice optimization also did not affect the XAS and XMCD spectra which are extended in a wide energy interval.

The details of the computational method are described in our previous papers, [16, 17] and here we only mention some aspects specific to the present calculations. The calculations were performed using the spin-polarized fully relativistic linear-muffin-tin-orbital (SPR LMTO) method [18, 19] for the experimentally observed lattice constants. For GeTe the lattice constant is  $a = 6.009$  Å, and for MnTe  $a = 4.125$  Å,  $c = 6.724$  Å [12]. We used the Perdew-Wang [20] parameterization for the exchange-correlation potential. Brillouin zone (BZ) integrations were performed using the improved tetrahedron method [21] and the charge was obtained self-consistently on a grid of 56  $\mathbf{k}$  points in the irreducible part of the BZ of  $(\text{Ge}_{1-x}\text{Mn}_x)\text{Te}$  for  $x = 0.03$  and 133  $\mathbf{k}$  points for  $x = 0.06$  and  $x = 0.125$ . To improve the potential we include additional empty spheres. The basis consisted of Mn, Ge and Te  $s$ ,  $p$ , and  $d$  LMTOs. Finally, the finite lifetime of a core hole was accounted for by folding the XAS and XMCD spectra with a Lorentzian. The widths of the core levels were taken from [22].

### 3. Results and discussion

#### 3.1. Energy band structure

Figure 2 presents the energy band structure and total density of states for pure MnTe and GeTe. Our LSDA calculations produce antiferromagnetic ground state for pure MnTe compound in agreement with the experiment [23, 24]. The DOS at the Fermi level was found to be very small. GeTe is a semiconductor with the experimentally measured energy gap of around 0.8 eV [25]. Our

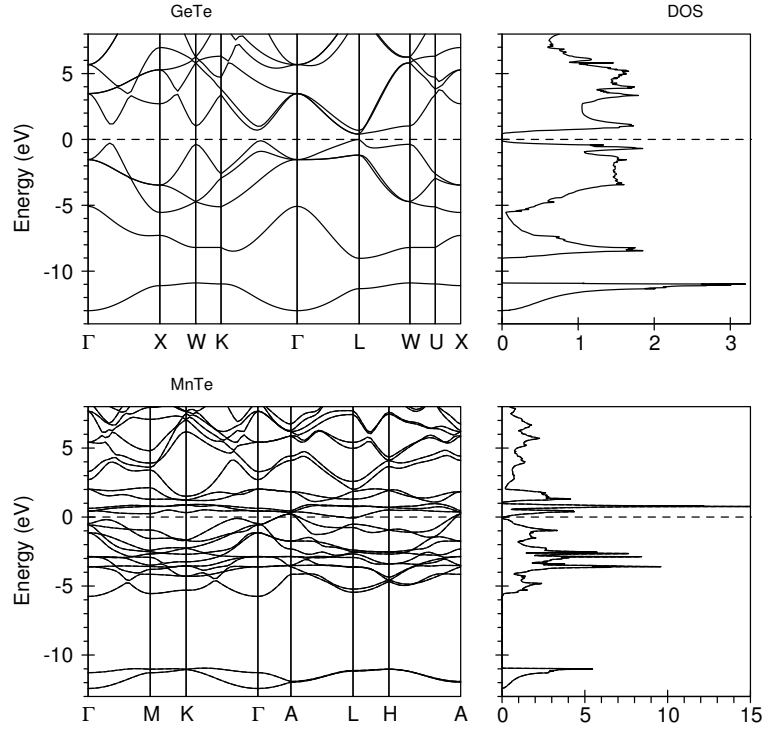


**Figure 2.** The energy band structure and total density of states [in states/(cell eV)] of the GeTe and MnTe. The Fermi energy is at zero.

LSDA calculations produce correct semiconductor ground state with underestimated energy gap of 0.40 eV. The non-muffin-tin correction to the crystal potential in the framework of CASTEP method improves the agreement with the experiment producing the gap of 0.6 eV [11]. However, the gap is still smaller than the experimentally measured one. This is typical of the calculations in the LSDA. To get a correct energy gap, one should take into account the Coulomb correlation in a proper way. The electronic correlations in Ge and Te  $p$  shells were treated in our calculations at the mean-field level using the LSDA+ $U$  approach [26] in its rotationally invariant implementation which is described in detail in our previous paper [27]. The exchange integral  $J$  was estimated from constrained LSDA calculations, and the values of 0.9 eV were used for the Ge and Te  $p$  states. The effective on-site Coulomb repulsion  $U$  was considered as an adjustable parameter. We used  $U = 3$  eV for the Ge and Te  $p$  states in GeTe to achieve good agreement with the experiment. The LSDA+ $U$  calculations produce the gap of 0.79 eV, while the experimentally measured one is equal to 0.8 eV [25].

Figure 3 presents the partial density of states for a 36-atom GeTe unit cell containing one  $\text{Mn}_{\text{Ge}}$  substitution ( $x = 0.03$ ) in the LSDA approximation. (Ge,Mn)Te DMS has the electronic structure of a semiconductor with direct energy gap at  $\Gamma$  symmetry point of 0.46 eV. The Te  $s$  states are located mostly at the  $-13.0$  to  $-10.8$  eV below the Fermi level and the  $s$  states of the Ge are situated at the  $-9.0$  eV to  $-5.2$  eV. The  $p$  states of the Ge and Te are strongly overlapped and occupy the  $-5.4$  to  $9.9$  eV energy range. The spin splitting of the Ge and Te  $4p$  states are quite small. The crystal splitting is not big at Mn site in (Ge,Mn)Te, and Mn  $d$  states of  $e_g$  and  $t_{2g}$  symmetry occupy almost the same energy interval  $-4.8$  to  $0$  for majority states and  $0.6$  to  $3.7$  eV for minority states. There is a strong hybridization between Mn  $3d$  and Ge and Te  $p$  states.

An important issue is the energy position of the  $3d$  states, which is usually solved by photoemission and x-ray bremsstrahlung isochromat (BIS) measurements. Figure 4 shows the experimental photoemission spectrum (PES) of (Ge,Mn)Te [7] compared with the calculated energy distribution for the occupied total DOS. The total DOS display correctly the main features of the experimental

photoemission spectrum. The PES consists of three major peaks. Peak *A* corresponds to the Mn *d* majority states, peaks *B* and *C* are to the *s* states of Ge and Te, respectively (see figure 3).

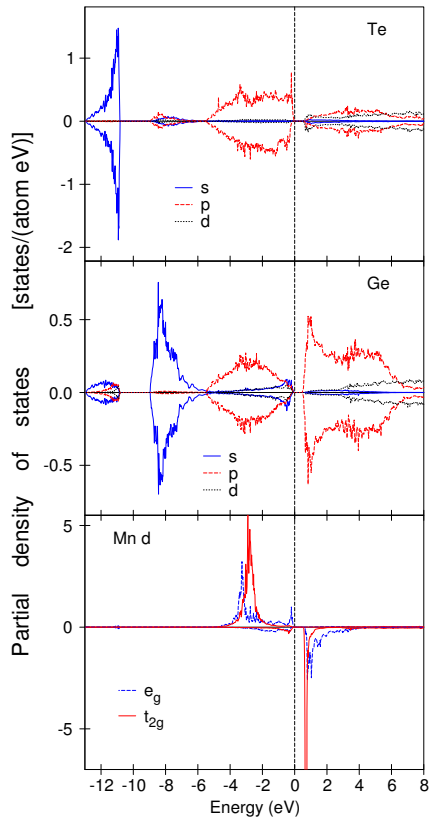


**Figure 3.** (Color online) The partial density of states [in states/(atom eV)] of the  $(\text{Ge}_{1-x}\text{Mn}_x)\text{Te}$  ( $x = 0.03$ ) in the LSDA approximation. The Fermi energy is at zero.

The magnetic moment of the  $(\text{Ge}_{1-x}\text{Mn}_x)\text{Te}$  is equal to  $5\mu_B$  for  $x = 0.03, 0.06$  and  $0.12$  in consistency with their semiconductor band structure. The LSDA calculations produce the energy gap equal to 0.46 eV, 0.34 eV and 0.27 eV for the concentration  $x = 0.03, 0.06$  and  $0.12$ , respectively. For the  $x = 0.5$  we obtain a semimetal solution with total magnetic moment  $\mu_{\text{total}} = 4.69\mu_B$ . Our band structure calculations produce the spin magnetic moment of  $3.466\mu_B$  at the  $\text{Mn}_{\text{Ge}}$  in the  $(\text{Ge}_{1-x}\text{Mn}_x)\text{Te}$  ( $x = 0.03$ ). The induced magnetic moments at the Te first neighbor sites are parallel to that of the Mn ions with spin magnetic moments about  $0.043\mu_B$ . Twelve Ge ions in the second neighbor shell couple ferromagnetically to the substituted Mn ion with spin magnetic moments of  $0.012\mu_B$ . The orbital moments at the Ge and Te sites are small with the largest one at the Te first neighbor sites ( $-0.001\mu_B$ ). The orbital magnetic moment at the  $\text{Mn}_{\text{Ge}}$  site is equal to  $0.055\mu_B$  and parallel to the spin moment.

The effect of Coulomb correlations on the electronic structure of the  $(\text{Ge},\text{Mn})\text{Te}$  was investigated using the rotationally invariant LSDA+*U* method [27, 28]. When  $U = 4$  eV is applied only to the Mn *d* states, its main effect is to increase the splitting between the occupied majority and unoccupied minority Mn *3d* states. This causes some increase of the energy gap, which became equal to 0.48 eV, 0.36 eV and 0.32 eV for the concentration  $x = 0.03, 0.06$  and  $0.12$ , respectively. For the  $x = 0.5$  the solution was found to be still semimetal.

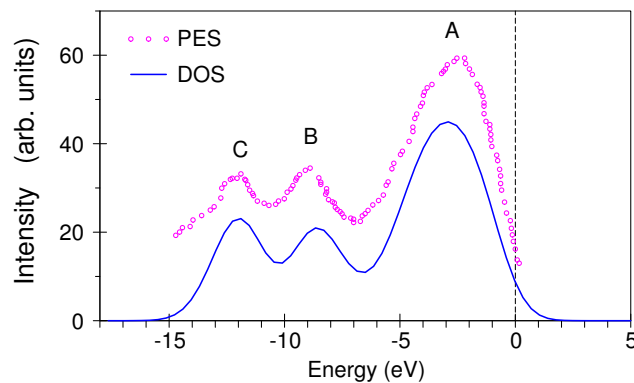


**Figure 4.** (Color online) The experimentally measured [7] (circles) PES in comparison with total DOS (full line) of  $(\text{Ge}_{1-x}\text{Mn}_x)\text{Te}$   $x = 0.03$ . The Fermi energy is at zero.

### 3.2. Mn $L_{2,3}$ XMCD spectra

Mn  $L_{2,3}$  x-ray absorption and magnetic circular dichroism study has been performed on ferromagnetic semiconductor  $(\text{Ge}_{1-x}\text{Mn}_x)\text{Te}$  with different Mn compositions  $x = 0.12, 0.32, 0.51,$  and  $1$  by Fukuma *et al.* [8, 9]. Clear XMCD signals are observed in all the  $(\text{Ge}_{1-x}\text{Mn}_x)\text{Te}$  except for  $x = 1$  due to the antiferromagnetic nature. Figure 5 presents the theoretically calculated isotropic XAS as well as XMCD spectra of  $(\text{Ge}_{1-x}\text{Mn}_x)\text{Te}$  at the Mn  $L_{2,3}$  edges in comparison with the experiment by Fukuma *et al.* [9]. The theory correctly describes the energy position and intensity of major  $L_3$  peak at  $\sim 640$  eV in the x-ray absorption and XMCD. We should mention here that a major shortcoming in our calculations is that the multiplet structure has not been included. Therefore, we fail to describe two high energy satellite structures in XAS at the  $642$  eV and  $644$  eV. The LSDA calculations also cannot produce the second high energy peak at the  $L_2$  edge at  $\sim 652$  eV both in the x-ray absorption and XMCD spectra. To calculate the shape of the multiplet spectra one has to use, for example, atomic calculations in Hartree-Fock approximation [29–31].

From our calculations we found that the shape of the XAS and XMCD spectra is almost independent of the concentration  $x$  in agreement with the experimental observation [9]. The results for  $x = 0.03$  and  $0.5$  are shown in figure 5. This implies that the magnetic order scarcely affects the local environment of the Mn atom: the local chemical environment of the ferromagnetically coupled Mn atoms is the same for  $(\text{Ge}_{1-x}\text{Mn}_x)\text{Te}$  with the wide range of  $x$ . We also found that the application of Hubbard repulsion  $U = 4$  eV at the Mn  $3d$  states hardly affects the Mn  $L_{2,3}$  XAS and XMCD spectra (not shown).

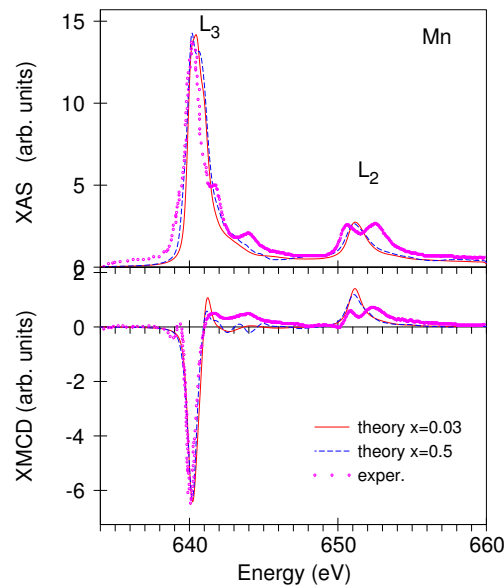


**Figure 5.** (Color online) Top panel: the experimentally measured [9] (circles) isotropic XAS of  $(\text{Ge}_{1-x}\text{Mn}_x)\text{Te}$  at the Mn  $L_{2,3}$  edges in comparison with the theoretically calculated for  $x = 0.03$  (full line) and  $x = 0.5$  (dashed line). Bottom panel: theoretically calculated for  $x = 0.03$  (full line) and  $x = 0.5$  (dashed line) and experimental [9] (circles) XMCD spectra at the Mn  $L_{2,3}$  edges.

## 4. Summary

We have studied the electronic structure and x-ray magnetic circular dichroism of the  $(\text{Ge},\text{Mn})\text{Te}$  diluted magnetic semiconductors by means of the *ab initio* fully-relativistic spin-polarized Dirac linear muffin-tin orbital method within the framework of the LSDA approximation as well as the

LSDA+ $U$  method. The x-ray magnetic circular dichroism spectra of (Ge,Mn)Te DMSs at the Mn  $L_{2,3}$  edges are investigated theoretically from first principles.

The  $(\text{Ge}_{1-x}\text{Mn}_x)\text{Te}$  for  $0.03 \leq x \leq 0.125$  has the electronic structure of a semiconductor with the magnetic moment of  $5\mu_B$  per unit cell. The LSDA calculations produce the energy gap equal to 0.46 eV, 0.34 eV and 0.27 eV for the concentrations  $x = 0.03, 0.06$  and  $0.12$ , respectively. For the  $x = 0.5$  we obtain a semimetal solution with the total magnetic moment  $\mu_{\text{total}} = 4.69\mu_B$ . Our band structure calculations produce the spin magnetic moment of  $3.466\mu_B$  at the  $\text{Mn}_{\text{Ge}}$  in the  $(\text{Ge}_{1-x}\text{Mn}_x)\text{Te}$  ( $x = 0.03$ ). The induced magnetic moments at the Te first neighbor sites are parallel to that of the Mn ions with spin magnetic moments about  $0.043\mu_B$ . Twelve Ge ions in the second neighbor shell couple ferromagnetically to the substituted Mn ion with spin magnetic moments of  $0.012\mu_B$ . The orbital moments at the Ge and Te sites are small with the largest one at the Te first neighbor sites ( $-0.001\mu_B$ ). The orbital magnetic moment at the  $\text{Mn}_{\text{Ge}}$  site is equal to  $0.055\mu_B$  and parallel to the spin moment.

The theory reasonably well produces the shape and energy positions of the major fine structures of the Mn XASs and XMCD spectra at the  $L_{2,3}$  edges. However, it does not produce two high energy satellite structures in XAS at the 642 eV and 644 eV at the  $L_3$  edge and the second high energy peak at the  $L_2$  edge at  $\sim 652$  eV. These multiplet structures need the treatment in Hartree-Fock approximation. From our calculations we found that the shape of the XAS and XMCD spectra is almost independent of the concentration  $x$  in agreement with the experimental observation. This implies that the magnetic order scarcely affects the local environment of the Mn atom: the local chemical environment of the ferromagnetically coupled Mn atoms is the same for  $(\text{Ge}_{1-x}\text{Mn}_x)\text{Te}$  with the wide range of  $x$ .

## Acknowledgements

V.N. Antonov gratefully acknowledges the hospitality at Max-Planck-Institut für Festkörperforschung in Stuttgart during his stay there. This work was supported by Science and Technology Center in Ukraine (STCU), Project No. 4930.

## References

1. Sanvito S., Theurich G., Hill N.A., J. Supercond., 2002, **15**, 85.
2. Jungwirth T., Sinova J., Masek J., Kucera J., MacDonald A.H., Rev. Mod. Phys., 2006, **78**, 809.
3. Ohno H., J. Magn. Magn. Mater., 1999, **200**, 110.
4. Fukuma Y., Murakami T., Asada H., Koyanagi T., Physica E, 2001, **10**, 273.
5. Fukuma Y., Arifuku M., Asada H., Koyanagi T., J. Appl. Phys., 2002, **91**, 7503.
6. Fukuma Y., Asada H., Miyashita J., Nishimura N., Koyanagi T., J. Appl. Phys., 2003, **93**, 7667.
7. Fukuma Y., Asada H., Koyanagi T., Appl. Physics Lett., 2006, **88**, 032507.
8. Sato H., Fujimoto, Fukuma Y., Tsuji K., Kimura A., Taniguchi M., Senba S., Tanaka A., Asada H., Koyanagi T., J. Electron. Spectrosc. Relat. Phenom., 2005, **144–147**, 727.
9. Fukuma Y., Sato H., Fujimoto K., Tsuji K., Kimura A., Taniguchi M., Senba S., Tanaka A., Asada H., Koyanagi T., J. Appl. Phys., 2006, **99**, 08D510.
10. Senba S., Fujimoto K., Sato H., Fukuma Y., Nakatake M., Arita M., Tsuji K., Asada H., Koyanagi T., Namatame H., Taniguchi M., J. Electron. Spectrosc. Relat. Phenom., 2005, **144–147**, 629.
11. Xie Z., Cheng W., Wu D., Lan Y., Huang S., Hu J., Shen J., J. Phys.: Condens. Matter, 2006, **18**, 7171.
12. Makovetskii G.I., Galyas A.I., Severin G.M., Yanushkevich K.I., J. Inorganic and Nuclear Chemistry, 1961, **19**, 229.
13. Blöchl P.E., Phys. Rev. B, 1994, **50**, 17953.
14. Perdew J.P., Burke K., Ernzerhof M., Phys. Rev. Lett., 1997, **78**, 1396.
15. Kresse G., Joubert J., Phys. Rev. B, 1999, **59**, 1758.
16. Antonov V.N., Dürr H.A., Kucherenko Y., Bekenov L.V., Yaresko A.N., Phys. Rev. B, 2005, **72**, 054441.
17. Antonov V.N., Jepsen O., Yaresko A.N., Shpak A.P., J. Appl. Phys., 2006, **100**, 043711.
18. Andersen O.K., Phys. Rev. B, 1975, **12**, 3060.

19. Nemoshkalenko V.V., Krasovskii A.E., Antonov V.N., Antonov V.N., Fleck U., Wonn H., Ziesche P., Phys. Status Solidi B, 1983, **120**, 283–296.
20. Perdew J., Wang Y., Phys. Rev. B, 1992, **45**, 13244–13249.
21. Blöchl P.E., Jepsen O., Andersen O.K., Phys. Rev. B, 1994, **49**, 16223.
22. Campbell J.L., Parr T., At. Data Nucl. Data Tables, 2001, **77**, 1–56.
23. Uchida E., Kondo H., Fukuota N., J. Phys. Soc. Jpn., 1956, **11**, 27.
24. Banewicz J.J., Heidelberg R.F., Luxem A.H., J. Phys. C, 1961, **65**, 615.
25. Park J.-W., Eom S.H., Lee H., Silva J. L. F.D., Lee Y.-S. K. T.-Y., Khang Y.H., Phys. Rev. B, 2009, **80**, 115209.
26. Anisimov V.I., Zaanen J., Andersen O.K., Phys. Rev. B, 1991, **44**, 943.
27. Yaresko A.N., Antonov V.N., Fulde P., Phys. Rev. B, 2003, **67**, 155103.
28. Liechtenstein A.I., Anisimov V.I., Zaanen J., Phys. Rev. B, 1995, **52**, R5467–R5470.
29. van der Laan G., Thole B.T., Sawatzky G.A., Goedkoop J.B., Fuggle J.C., Esteve J.M., Karnatak R.C., Remeika J.P., Dabkowska H.A., Phys. Rev. B, 1986, **34**, 6529.
30. de Groot F. M.F., Fuggle J.C., Thole B.T., Sawatzky G.A., Phys. Rev. B, 1990, **42**, 5459.
31. van Elp J., Potze R.H., Esker H., Berger R., Sawatzky G.A., Phys. Rev. B, 1992, **44**, 1530.

## **Електронна структура та рентгенівський магнітний циркулярний дихроїзм у розбавлених магнітних напівпровідниках (Ge,Mn)Te**

В.Н. Антонов<sup>1,2</sup>, А.П. Шпак<sup>1</sup>, Л.В. Бекенов<sup>1</sup>, Л.П. Гермаш<sup>3</sup>, А.Н. Ярьсько<sup>2</sup>

<sup>1</sup> Інститут металофізики ім. Курдюмова НАН України, бульвар Академіка Вернадського, 36, Київ 03680, Україна

<sup>2</sup> Інститут дослідження твердого тіла тов. Макса Планка, Гайзенбергштрассе 1, D–70569 Штутгарт, Німеччина

<sup>3</sup> Національний технічний університет України “Київський політехнічний інститут”, вул. Політехнічна 14, Київ 03056, Україна

На основі розрахунків повністю релятивістським діраківським лінійним методом MT-орбіталей (LM-TO) теоретично з перших принципів досліджено електронну структуру розбавлених магнітних напівпровідників (Ge,Mn)Te. Розрахунки проведено як у наближенні локальної спінової густини (LSDA), так і методом LSDA+*U*. Теоретично з перших принципів досліджено Mn  $L_{2,3}$  спектри рентгенівського магнітного циркулярного дихроїзму (PMCD) в сполуці (Ge,Mn)Te. Вивчено походження спектрів PMCD. Результати розрахунків порівняно з наявними експериментальними даними.

**Ключові слова:** електронна структура, розбавлені магнітні напівпровідники, рентгенівський магнітний циркулярний дихроїзм